

Electrochemical lithiation of Ti_5M_3 , Ti_3M and Zr_3M ($M = Sn, Sb$) binary intermetallics

Vasyl KORDAN^{1*}, Oksana ZELINSKA¹, Volodymyr PAVLYUK¹, Igor OSHCHAPOVSKY¹, Roman SERKIZ²

¹ Department of Inorganic Chemistry, Ivan Franko National University of Lviv, Kyryla i Mefodiya St. 6, 79005 Lviv, Ukraine

² Scientific-Technical and Educational Centre of Low Temperature Studies, Ivan Franko National University of Lviv, Drahomanova St. 50, 79005 Lviv, Ukraine

* Corresponding author. E-mail: kordan50@gmail.com

Received June 16, 2016; accepted June 29, 2016; available on-line November 7, 2016

The binary phases Ti_5M_3 , Ti_3M and Zr_3M ($M = Sn, Sb$) were studied for electrochemical lithiation, using powder X-ray diffraction, scanning electron microscopy (SEM) and energy-dispersive X-ray analysis (EDX). The investigation showed that the morphology of the cathode and the anode surfaces undergo changes, and the grain size of the materials decreases. The phase analysis of the anode materials revealed that the Ti_5Sn_3 (structure type Mn_5Si_3) and Ti_3Sn (structure type Mg_3Cd) phases form solid solutions by insertion of Li atoms into the initial structure. The insertion is reversible. The phases Ti_5Sb_3 (structure type Y_5Bi_3), Ti_3Sb , Zr_3Sn (structure type Cr_3Si), and Zr_3Sb (structure type Ni_3P) form solid solutions by substitution of Li for Sn or Sb atoms. Only the Zr_3Sb phase showed weakly reversible substitution. Among the investigated compounds, the most suitable structure types for intercalation of lithium appeared to be the Mn_5Si_3 - and Mg_3Cd -types, where the Li atoms occupy octahedral voids. The intermetallic compounds containing tin showed better ability for electrochemical lithiation than the compounds containing antimony. This can be explained by the easier interaction of antimony and lithium with the formation of binary compounds.

Intermetallic compound / Electrochemical lithiation / Li-ion battery

1. Introduction

Electrode materials on the basis of intermetallic compounds are widely used in the production of modern energy sources. Many scientists actively study the ability of these materials to intercalate and store hydrogen or lithium [1,2]. Intermetallic compounds containing *d*- and *p*-elements have the ability to intercalate lithium atoms in their structures, and can be used as materials for negative electrodes. The main requirement for these electrode materials is the availability of large octahedral voids in their structures.

Among the binary title compounds, the phase Ti_5Sn_3 has a hexagonal structure (Mn_5Si_3 -type), the phase Ti_5Sb_3 an orthorhombic structure (Yb_5Bi_3 -type), Ti_3Sn a hexagonal structure (Mg_3Cd -type), Zr_3Sb a tetragonal structure (Ni_3P -type), Ti_3Sb and Zr_3Sn cubic structures (Cr_3Si -type). The authors of [3] observed concentration-induced polymorphism for Ti_3Sb . They suggested that the phase $Ti_{3.2}Sb_{0.8}$ crystallizes in a hexagonal Mg_3Cd -type structure. The results of the phase analysis of a $Ti_{80}Sb_{20}$ alloy did not confirm the formation of the hexagonal phase.

Lithium intermetallic compounds containing B, Al, C, Si, Ge, Sn, Pb, or Sb have been intensively investigated as possible anode materials for lithium-ion batteries. The disadvantages of these electrodes are limited cycle stability and electrode lifetime [4-8].

The binary phases La_5Ge_3 , La_5Sn_3 , Gd_5Ge_3 , and Gd_5Sn_3 crystallize in hexagonal Mn_5Si_3 -type structures and form solid solutions of the inclusion type, with homogeneity ranges of up to 0.4-0.5 Li atoms per formula unit. The Li atoms occupy the position *2b* and the structure changes to the Hf_5CuSn_3 -type without changing the symmetry [9]. The binary phases Zr_5Sn_3 , Gd_5Sn_3 , and Y_5Sn_3 also form inclusion-type solid solutions with Hf_5CuSn_3 -type structures [10,11]. Electrode materials on the basis of $Zr_3Sn_3Li_x$ provide a reversible specific capacity of 140-160 mA·h/g. Intercalation of Li is often accompanied by reactions of substitution-decomposition. In [10,11] the formation of intermediate phases containing tin and lithium, such as $Li_{17}Sn_4$ ($Li_{17}Pb_4$ structure type), was observed. After the electrochemical lithiation, the matrix of the material became defective and Li atoms substituted for some Sn atoms. In the case of lithiation of pure tin,

Li_5Sn_2 (own structure type) was obtained [12]. Hence, the nature of the metallic matrix affects the formation of intermediate phases.

In the present work we decided to synthesise the Ti_5M_3 , Ti_3M , and Zr_3M ($M = Sn, Sb$) phases and study their electrochemical lithiation, with the purpose to search for suitable structures for electrochemical intercalation of lithium, and investigate the influence of the p -element on these processes and application in Li-ion batteries.

2. Experimental

Titanium, zirconium, tin, and antimony, with a nominal purity of more than 99.9 wt.%, were used as starting materials for the synthesis of the alloys. Samples with the nominal compositions $Ti_{62.5}Sn_{37.5}$, $Ti_{62.5}Sb_{37.5}$, $Ti_{75}Sn_{25}$, $Ti_{75}Sb_{25}$, $Zr_{75}Sn_{25}$, and $Zr_{75}Sb_{25}$, were prepared by arc melting. The alloys were annealed in silica ampoules at 400°C for 2 months with final quenching in cold water.

The morphology of the material surfaces, and the qualitative and quantitative phase compositions of the alloys, were studied before and after the electrochemical processes, by powder X-ray diffraction (powder diffractometer DRON-2.0M, Fe $K\alpha$ -radiation) and EDX-analysis (scanning electron microscope REMMA 102-02). Unit cell refinements were performed with the Latcon and PowderCell programs [13,14].

Electrochemical insertion of lithium into the binary phases Ti_5M_3 and Ti_3M was carried out in Swagelok-type cells that consisted of a negative electrode containing 0.3-0.4 g of the alloy and a positive electrode containing $LiCoO_2$. A separator, soaked in electrolyte (1 M solution of $LiPF_6$ in ethylenecarbonate / dimethylcarbonate), was placed between the electrodes. Testing of the batteries was carried out in the galvanostatic regime (0.2-0.5 mA) over 30 cycles. A galvanostat MTech G410-2 [15] was used to measure the electrochemical characteristics of the batteries.

3. Results and discussion

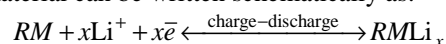
Careful analysis of the powder patterns of $Ti_{62.5}M_{37.5}$, $Ti_{75}M_{25}$, and Zr_3M before lithiation (see Table 1) showed that all the samples contained the expected phases, and less than 5 % of by-products, which fortunately did not interfere with the electrochemical investigation of the main phases. Analysis of the samples after electrochemical lithiation revealed that the phases Ti_5Sn_3 (structure type Mn_5Si_3) and Ti_3Sn (structure type Mg_3Cd) had formed inclusion-type solid solutions, due to the intercalation of lithium atoms into the voids of the initial structures (the lattice parameters of the main phase had increased after lithiation) [16]. On the contrary, Ti_5Sb_3 (structure type

Y_5Bi_3), Ti_3Sb , Zr_3Sn (structure type Cr_3Si), and Zr_3Sb (structure type Ni_3P) had formed solid solutions by substitution of lithium for the p -element (the lattice parameters of the main phases had decreased after lithiation).

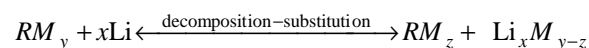
It should be noticed that the sample $Ti_{62.5}Sn_{37.5}$ contained the hexagonal β - Ti_6Sn_5 phase (own structure type) as secondary phase. However, after annealing at 400°C the formation of the orthorhombic α - Ti_6Sn_5 (structure type Nb_6Sn_5) is expected [17,18]. We believe that β - Ti_6Sn_5 is stabilized by admixtures and the polymorphic transformation β - $Ti_6Sn_5 \leftrightarrow \alpha$ - Ti_6Sn_5 becomes impossible. The sample $Ti_{62.5}Sb_{37.5}$ contained the orthorhombic $Ti_{10.84}Sb_{7.73}$ phase (structure type $Cr_{11}Ge_8$) as a secondary phase. This phase also forms a solid solution by substitution. The change of the cell volume due to Li-intercalation reached ~1 %, while for the main phase Ti_5Sb_3 it was ~1.6 %. The samples of composition $Ti_{75}Sn_{25}$ and $Zr_{75}Sn_{25}$ were also not single-phase. The largest change of the cell volume was ~1.6 % for Zr_3Sb (structure type Ni_3P).

As shown in Table 1, the change of the cell volume of the Ti_5Sn_3 phase was not significant. This may be explained assuming that the inclusion of lithium atoms into octahedral voids in Wyckoff position $2b$ is accompanied by partial replacement of Sn-atoms of the material structure by Li-atoms. This is possible when the octahedral voids have sufficient volume. After maximal saturation by Li, the original structure was destroyed. As a result, an intermediate phase of tin and lithium with the composition $Li_{17}Sn_4$ (structure type $Li_{17}Pb_4$) was formed. A similar situation was observed when the electrode material contained Sb. Partial replacement of Sb atoms by Li atoms led to the formation of intermediate phases of lithium with antimony, such as α - Li_3Sb , β - Li_3Sb , and Li_2Sb .

The electrochemical reaction of intercalation of lithium into the initial structure of the electrode material can be written schematically as:



The electrochemical reaction of substitution by lithium and the formation of intermediate phases can be written as:



It follows that, if the formation of intermediate phases of lithium with p -elements is observed after the electrochemical lithiation, the original binary phases form limited solid solutions of substitution and the lattice parameters of the new phases decrease.

Fig. 1 shows the change in the morphology of the surfaces and the reduction of the grain size resulting from the electrochemical processes. After intercalation of Li atoms into the original structure, the lattice parameters had increased, but the atomic ratio Ti/Zr : Sn/Sb had not changed (see Fig. 1g,h). In the case of substitution of Li for p -element atoms

Table 1 Qualitative and quantitative composition of the negative electrode materials, before and after the electrochemical lithiation.

Composition of the alloys	Results of the phase analysis	
	before lithiation	after lithiation
$Ti_{62.5}Sn_{37.5}$	<p>Ti_5Sn_3 (structure type Mn_5Si_3, space group $P6_3/mcm$) $a = 7.996(3) \text{ \AA}$, $c = 5.420(3) \text{ \AA}$, $V = 300.1(2) \text{ \AA}^3$;</p> <p>$\beta$-$Ti_6Sn_5$ (traces) (structure type Ti_6Sn_5, space group $P6_3/mmc$) $a = 9.210(2) \text{ \AA}$, $c = 5.697(2) \text{ \AA}$, $V = 418.6(2) \text{ \AA}^3$;</p> <p>$\alpha$-Ti (traces) (structure type Mg, space group $P6_3/mmc$) $a = 2.940(6) \text{ \AA}$, $c = 4.696(1) \text{ \AA}$, $V = 35.10(5) \text{ \AA}^3$</p>	<p>$Ti_5Sn_3Li_x$ (structure type Hf_5CuSn_3, space group $P6_3/mcm$) $a = 8.009(1) \text{ \AA}$, $c = 5.426(1) \text{ \AA}$, $V = 301.4(1) \text{ \AA}^3$;</p> <p>$\beta$-$Ti_6Sn_5$ (traces) (structure type Ti_6Sn_5, space group $P6_3/mmc$) $a = 9.222(2) \text{ \AA}$, $c = 5.700(3) \text{ \AA}$, $V = 419.8(2) \text{ \AA}^3$;</p> <p>$\alpha$-Ti (traces) (structure type Mg, space group $P6_3/mmc$) $a = 2.966(1) \text{ \AA}$, $c = 4.710(2) \text{ \AA}$, $V = 35.90(1) \text{ \AA}^3$;</p> <p>$Li_{17}Sn_4$ (traces) (structure type $Li_{17}Pb_4$, space group $F-43m$) $a = 19.743(6) \text{ \AA}$, $V = 769.56(6) \text{ \AA}^3$</p>
$Ti_{62.5}Sb_{37.5}$	<p>Ti_5Sb_3 (structure type Y_5Bi_3, space group $Pnma$) $a = 10.169(9) \text{ \AA}$, $b = 8.342(2) \text{ \AA}$, $c = 7.146(1) \text{ \AA}$, $V = 606.2(7) \text{ \AA}^3$;</p> <p>$Ti_{10.84}Sb_{7.73}$ (traces) (structure type $Cr_{11}Ge_8$, space group $Pnma$) $a = 14.86(4) \text{ \AA}$, $b = 5.572(9) \text{ \AA}$, $c = 17.64(4) \text{ \AA}$, $V = 1462(3) \text{ \AA}^3$</p>	<p>$Ti_5Sb_{3-x}Li_x$ (structure type Y_5Bi_3, space group $Pnma$) $a = 10.17(1) \text{ \AA}$, $b = 8.21(2) \text{ \AA}$, $c = 7.14(2) \text{ \AA}$, $V = 596.6(9) \text{ \AA}^3$;</p> <p>$Ti_{10.84}Sb_{7.73}Li_x$ (traces) (structure type $Cr_{11}Ge_8$, space group $Pnma$) $a = 14.62(2) \text{ \AA}$, $b = 5.596(3) \text{ \AA}$, $c = 17.69(3) \text{ \AA}$, $V = 1448(2) \text{ \AA}^3$</p>
$Ti_{75}Sn_{25}$	<p>Ti_3Sn (structure type Mg_3Cd, space group $P6_3/mmc$) $a = 5.901(1) \text{ \AA}$, $c = 4.745(1) \text{ \AA}$, $V = 143.09(7) \text{ \AA}^3$;</p> <p>$\alpha$-Ti (traces) (structure type Mg, space group $P6_3/mmc$) $a = 2.949(1) \text{ \AA}$, $c = 4.709(2) \text{ \AA}$, $V = 35.49(2) \text{ \AA}^3$</p>	<p>Ti_3SnLi_x (structure type Mg_3Cd, space group $P6_3/mmc$) $a = 5.922(2) \text{ \AA}$, $c = 4.749(1) \text{ \AA}$, $V = 144.28(8) \text{ \AA}^3$;</p> <p>$\alpha$-Ti (traces) (structure type Mg, space group $P6_3/mmc$) $a = 2.947(1) \text{ \AA}$, $c = 4.723(2) \text{ \AA}$, $V = 35.52(2) \text{ \AA}^3$</p>
$Ti_{75}Sb_{25}$	<p>Ti_3Sb (structure type Cr_3Si, space group $Pm-3n$) $a = 5.214(1) \text{ \AA}$, $V = 141.77(10) \text{ \AA}^3$</p>	<p>$Ti_3Sb_{1-x}Li_x$ (structure type Cr_3Si, space group $Pm-3n$) $a = 5.206(2) \text{ \AA}$, $V = 141.10(1) \text{ \AA}^3$;</p> <p>$\alpha$-$Li_3Sb$ (traces) (structure type BiF_3, space group $Fm-3m$) $a = 6.553 \text{ \AA}$, $V = 281.4(3) \text{ \AA}^3$;</p> <p>$Li_2Sb$ (traces) (structure type Mg_2Ga, space group $P-62c$) $a = 7.989(5) \text{ \AA}$, $c = 6.526(9) \text{ \AA}$, $V = 360.7(6) \text{ \AA}^3$</p>
$Zr_{75}Sn_{25}$	<p>Zr_3Sn (structure type Cr_3Si, space group $Pm-3n$) $a = 5.623 \text{ \AA}$, $V = 177.8(2) \text{ \AA}^3$;</p> <p>$Zr_5Sn_3$ (traces) (structure type Mn_5Si_3, space group $P6_3/mcm$) $a = 8.450(3) \text{ \AA}$, $c = 5.772(3) \text{ \AA}$, $V = 356.9(3) \text{ \AA}^3$</p>	<p>$Zr_3Sn_{1-x}Li_x$ (structure type Cr_3Si, space group $Pm-3n$) $a = 5.613(3) \text{ \AA}$, $V = 176.8(2) \text{ \AA}^3$;</p> <p>$Zr_5Sn_3Li_x$ (traces) (structure type Mn_5Si_3, space group $P6_3/mcm$) $a = 8.468(3) \text{ \AA}$, $c = 5.801(2) \text{ \AA}$, $V = 360.3(3) \text{ \AA}^3$</p>
$Zr_{75}Sb_{25}$	<p>Zr_3Sb (structure type Ni_3P, space group $I-4$) $a = 11.319(4) \text{ \AA}$, $c = 5.662(3) \text{ \AA}$, $V = 725.5(5) \text{ \AA}^3$</p>	<p>$Zr_3Sb_{1-x}Li_x$ (structure type Ni_3P, space group $I-4$) $a = 11.258(5) \text{ \AA}$, $c = 5.630(3) \text{ \AA}$, $V = 713.7(5) \text{ \AA}^3$;</p> <p>$\beta$-$Li_3Sb$ (traces) (structure type Na_3As, space group $P6_3/mmc$) $a = 4.733(3) \text{ \AA}$, $c = 8.23(1) \text{ \AA}$, $V = 159.8(3) \text{ \AA}^3$</p>

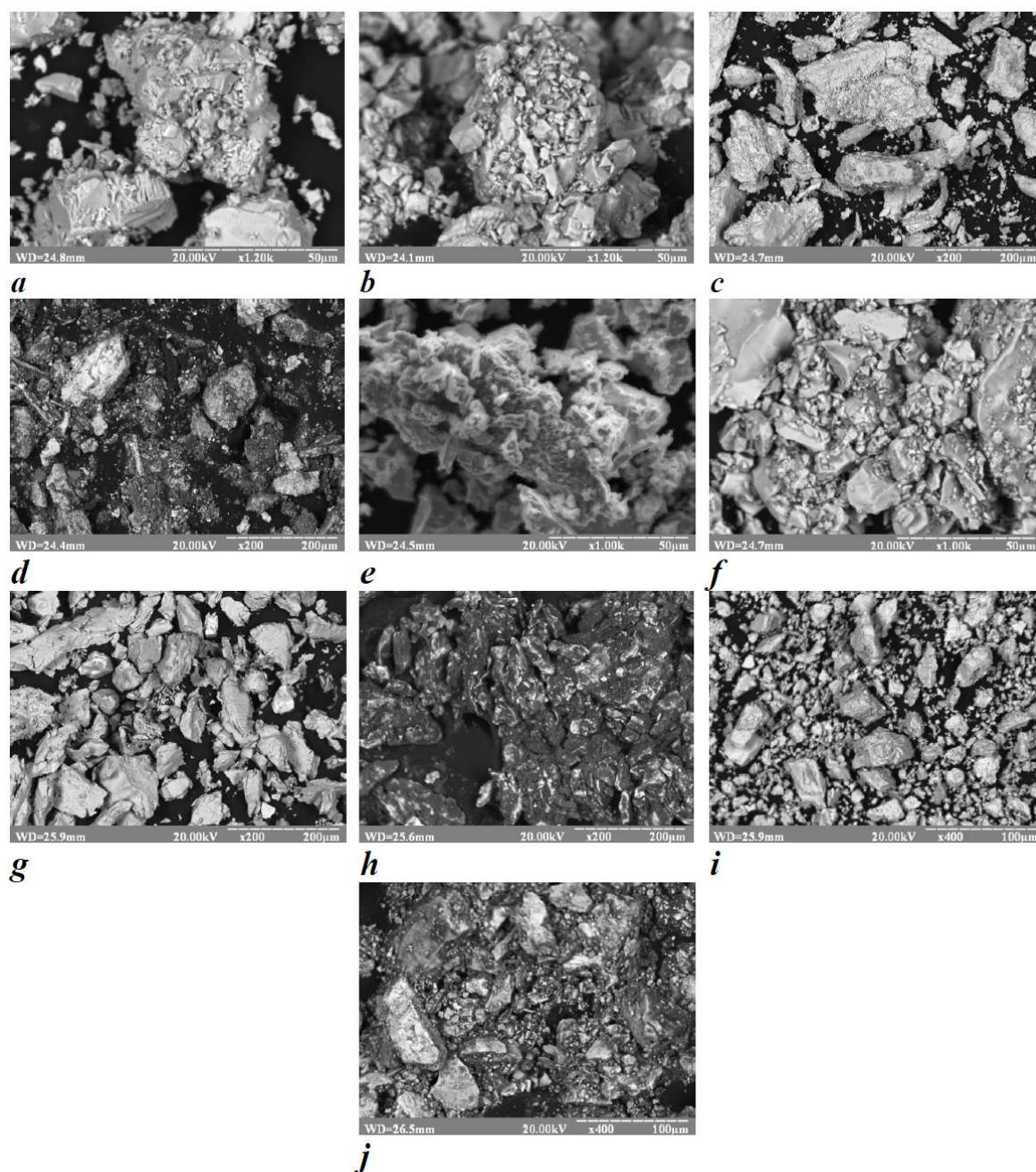


Fig. 1 SEM-images of anode materials based on the title compounds with the following compositions: $Ti_{60.78}Sb_{39.22}$ (a), $Ti_{62.13}Sb_{37.86}$ (b), $Zr_{77.33}Sn_{22.67}$ (c), $Zr_{77.61}Sn_{22.39}$ (d), $Ti_{74.15}Sb_{25.85}$ (e), $Ti_{74.94}Sb_{25.06}$ (f), $Ti_{75.64}Sn_{24.36}$ (g), light phase – $\sim Ti_{69.32}Sn_{22.33}Li_{8.35}$, dark phase – $\sim Ti_{11.05}Sn_{3.96}P_{3.99}F_{40.96}O_{40.04}$ (h), $Zr_{76.39}Sb_{23.61}$ (i), $Zr_{77.11}Sb_{22.89}$ (j), before and after 30 cycles of electrochemical lithiation.

a change of the Ti/Zr : Sn/Sb ratio towards a larger amount of *d*-elements was observed (see Fig. 1a-f,i,j). The results of the EDX-analysis revealed the formation of Li-based intermetallics. For one of them the composition was determined as $Ti_{69.32}Sn_{22.33}Li_{8.35}$ (the amount of Li was calculated as 100 % minus the amounts of Ti and Sn). Decomposition of the electrolyte and the formation of the solid electrolyte interface (SEI) $Ti_{11.05}Sn_{3.96}P_{3.99}F_{40.96}O_{40.04}$ were assumed at a potential of 5 V.

We also studied the change of the structure of $LiCoO_2$, which was used as material for the positive electrode, using X-ray diffraction, SEM and EDX-analysis. The structure of the original oxide had rhombohedral symmetry and belonged to the $NaFeO_2$ -type (space group $R-3m$, $a = 2.8444(6)$ Å, $c = 14.115(3)$ Å).

During electrochemical delithiation of $LiCoO_2$ a change of the original structure takes place. During the first cycles of delithiation, part of the Li atoms leave

the position $3a$. This is possible due to the location of Li atoms in interlayers of the structure (see Fig. 2). When the cathode material LiCoO_2 has given off more than 0.32 lithium atoms per formula unit, the structure transforms into disordered $\text{Li}_{0.68}\text{CoO}_2$ having the same symmetry (space group $R\bar{3}m$), but the lattice parameter c is twice as large [19]. The formation of $\text{Li}_{0.68}\text{CoO}_2$ was first observed after the 10-th charge-discharge cycle. This phase is also electrochemically active. The unit cell lattice parameters had decreased after delithiation: $a = 2.815(9) \text{ \AA}$, $c = 29.33(1) \text{ \AA}$, $V = 201.4(1) \text{ \AA}^3$ (after 10 cycles), $a = 2.780(1) \text{ \AA}$, $c = 29.32(1) \text{ \AA}$, $V = 196.3(1) \text{ \AA}^3$ (after 30 cycles). Fig. 3 shows the dynamics of the reduction of the grain size and the change in the morphology of the surfaces of the cathode material on a number of the cycle.

During the electrochemical lithiation, the amount of lithium that comes out of the channels gradually increases. This is due to the intercalation of lithium atoms into voids of the original structure and the formation of intermediate lithium-containing phases. When the amount of Li is reduced, the lattice parameters of the cathode material decrease. The dependence of the lattice parameters on the number of cycles is presented in Table 2.

The Ti_5Sn_3 and Ti_3Sn phases showed satisfactory results regarding electrochemical insertion of Li. The main causes of the reduction of the capacity of the $\text{LiCoO}_2 / \text{Ti}_5\text{Sn}_3$ (Ti_3Sn) prototype batteries may be

attributed to the formation of dendrites and interaction of the electrode material with the electrolyte. The formation of a passivation film impedes the lithiation process and the battery breaks down. This can explain the significant decrease of the discharging time with the number of cycles. Charge-discharge curves for $\text{LiCoO}_2 / \text{Ti}_5\text{Sn}_3$ (Ti_3Sn) are shown in Fig. 4. The nominal discharge voltage of the system $\text{LiCoO}_2 / \text{Ti}_5\text{Sn}_3$ was 1.3 V, for $\text{LiCoO}_2 / \text{Ti}_3\text{Sn}$ it was 1.35 V.

The coordination polyhedron of the Li atoms in $\text{Ti}_5\text{Sn}_3\text{Li}_x$ is an octahedron $[\text{LiTi}_6]$ (Fig. 5a), while the coordination polyhedron of the Li atoms in Ti_3SnLi_x is a strongly deformed octahedron $[\text{LiTi}_4\text{Sn}_2]$ (Fig. 5b).

The charge curves of the first cycles (Fig. 4a,c) point on a process of surface and volume activation of the materials. When the activation was finished, the potential of the charging plateau had increased to $\sim 3 \text{ V}$.

The formation of a limited solid solution by substitution on the basis of Zr_3Sb is a complex process that is associated with various activation processes. The different kinds of plateau and their different potential from cycle to cycle confirm this (Fig. 6). When the Li atoms penetrate the structure, they replace Sb and form a substitution solid solution $\text{Zr}_3\text{Sb}_{1-x}\text{Li}_x$ and the binary phase $\beta\text{-Li}_3\text{Sb}$ as a by-product. The homogeneity range of the solid solution is very small. The processes of lithiation-delithiation are reversible.

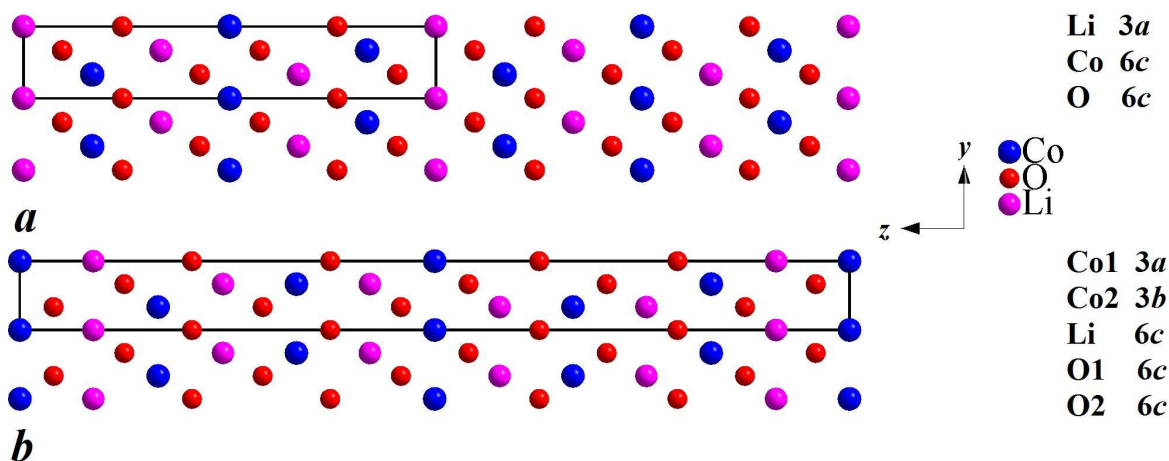


Fig. 2 Projections of the unit cells of LiCoO_2 (a) and $\text{Li}_{0.62}\text{CoO}_2$ (b).

Table 2 Lattice parameters of LiCoO_2 as a function of the number of charge-discharge cycles.

Number of cycle	Lattice parameters of the cathode material			
	$a, \text{ \AA}$	$c, \text{ \AA}$	$V, \text{ \AA}^3$	$\Delta V/V, \%$
before delithiation	2.8444(6)	14.115(3)	98.90(4)	–
5-th	2.8138(3)	14.040(2)	96.27(2)	2.66
10-th	2.8122(5)	14.034(3)	96.12(4)	2.81
15-th	2.8101(5)	13.996(6)	95.72(4)	3.22
20-th	2.8088(9)	13.973(7)	95.47(6)	3.47
30-th	2.8132(6)	13.813(8)	94.67(5)	4.28

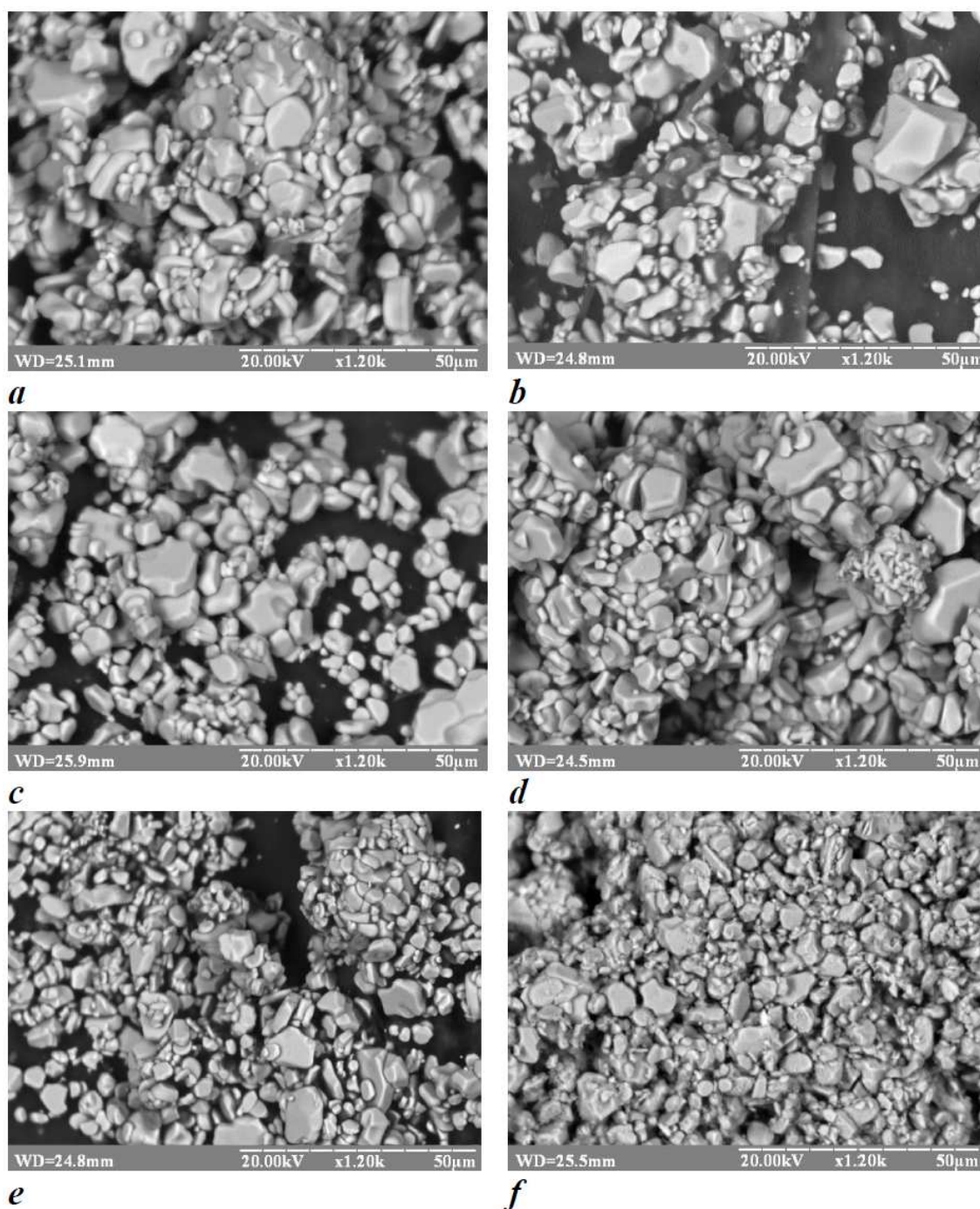


Fig. 3 SEM-images of the initial $LiCoO_2$ cathode material (a) and after the 5-th (b), 10-th cycle (c), 15-th (d), 20-th (e), and 30-th (f) cycle.

Comparing the formation of solid solutions by thermal and electrochemical methods, the following generalizations can be made. When lithium is intercalated electrochemically into the structure of an intermetallic compound, the formation of limited solid solutions by inclusion or replacement of p -elements (Sn, Sb) by Li is observed. Among the solid solutions formed by thermal methods, mainly solid solutions with substitution of Li for d -elements are observed [20,21].

4. Conclusions

Based on the electrochemical lithiation of the binary intermetallic compounds Ti_5M_3 , Ti_3M , and Zr_3M ($M = Sn, Sb$), we came to the conclusion that the nature of the p -element plays a dominant role in this process, besides the size of the voids. The phases Ti_5Sn_3 (structure type Mn_5Si_3) and Ti_3Sn (structure type Mg_3Cd) form limited solid solutions by insertion of Li atoms. The phases Ti_5Sb_3 (structure type Y_5Bi_3),

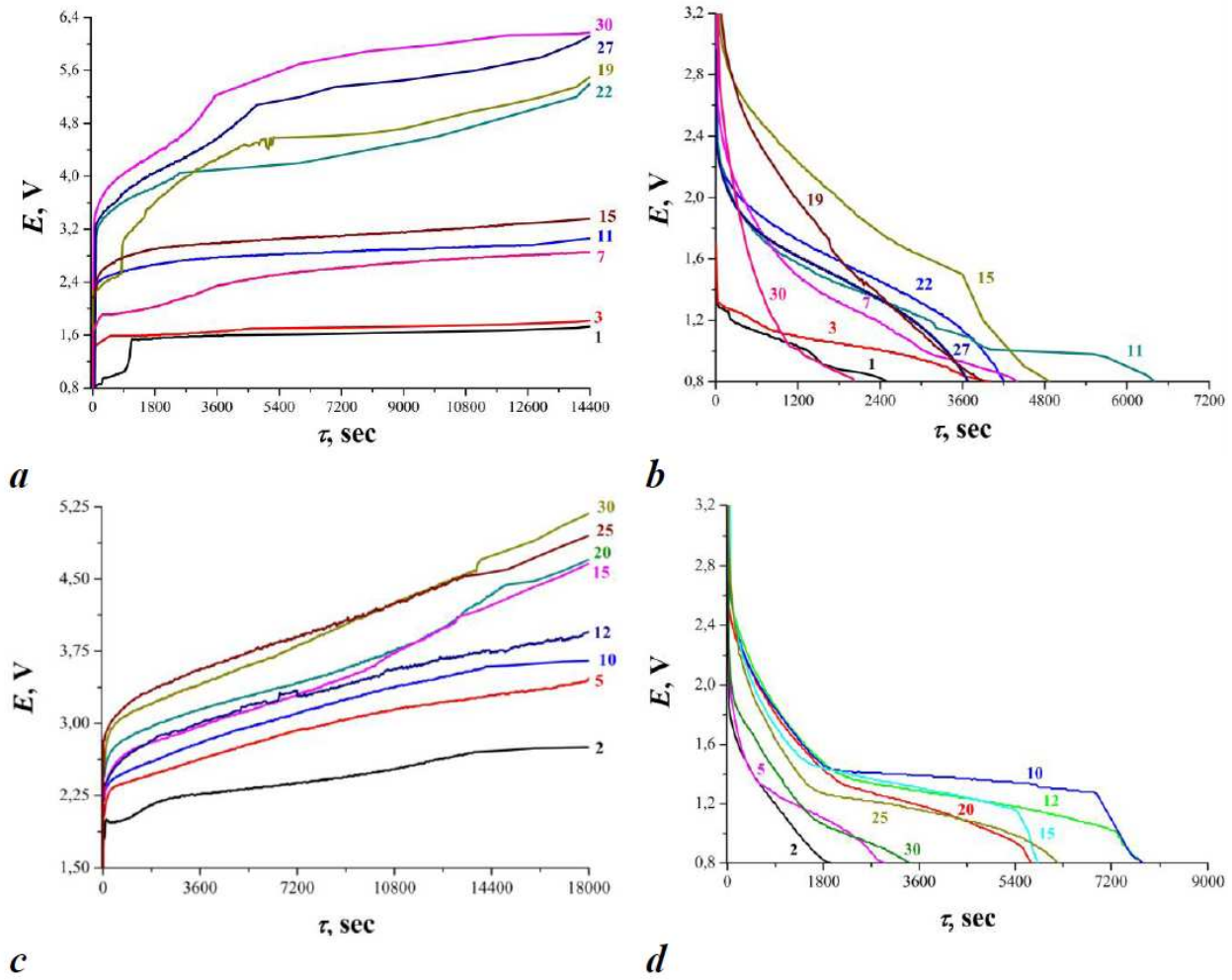


Fig. 4 Charge-discharge curves for $LiCoO_2 / Ti_3Sn$ (*a, b*) and $LiCoO_2 / Ti_5Sn_3$ (*c, d*) batteries (charge at 0.5 mA, discharge at 0.2 mA).

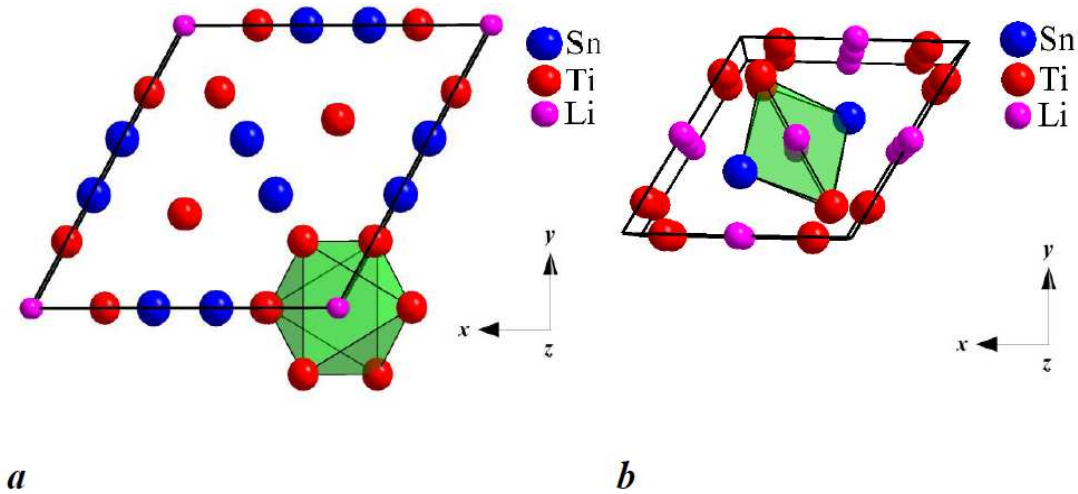


Fig. 5 Projection of the unit cells of $Ti_5Sn_3Li_x$ (*a*) and Ti_3SnLi_x (*b*).

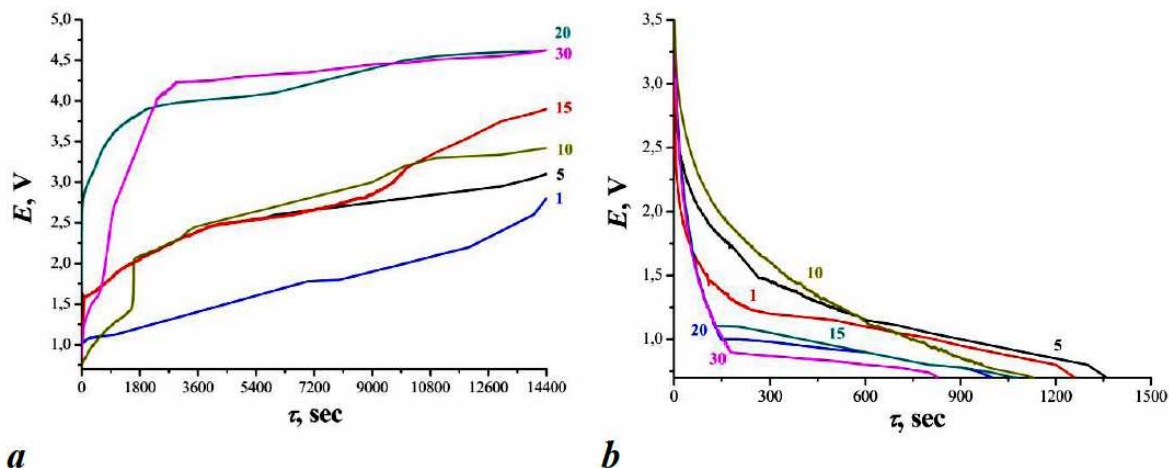


Fig. 6 Charge-discharge curves for the $LiCoO_2 / Zr_3Sb$ battery, charge at 0.5 mA (a), discharge at 0.2 mA (b).

Ti_3Sb , Zr_3Sn (structure type Cr_3Si), and Zr_3Sb form solid solutions by substitution of Li atoms for Sn or Sb. The intermetallic compounds containing tin showed better ability for electrochemical lithiation than the compounds containing antimony. This can be explained by the easier interaction of antimony and lithium, with the formation of binary compounds.

References

- [1] J.O. Besenhard, *Handbook of Battery Materials*, Wiley-VCH, Weinheim, 1999.
- [2] C.A. Vincent, B. Scrosati, *Modern Batteries: An Introduction to Electrochemical Power Sources*, 2nd edition, Arnold, London, 1997.
- [3] H. Nowotny, R. Funk, J. Pesl, *Monatsh. Chem.* 82 (1951) 513-525.
- [4] V.V. Pavlyuk, O.I. Bodak, In: G. Effenberg, F. Aldinger, A. Prince (Eds.), *Ternary Alloys – Evaluated Constitutional Data, Phase Diagrams, Crystal Structures and Applications of Lithium Alloy Systems*, VCH, Weinheim, 1995.
- [5] R. Pöttgen, T. Dinges, H. Eckert, P. Sreeraj, H.-D. Wiemhöfer, *Z. Phys. Chem.* 224 (2010) 1475-1504.
- [6] B. Scrosati, J. Garche, *J. Power Sources* 195 (2010) 2419-2430.
- [7] W.J. Zhang, *J. Power Sources* 96 (2011) 13-24.
- [8] T. Langer, S. Dupke, C. Dippel, H. Eckert, R. Pöttgen, *Z. Naturforsch. B* 67 (2012) 1212-1220.
- [9] A. Stetskiv, V. Kordan, I. Tarasiuk, O. Zelinska, V. Pavlyuk, *Chem. Met. Alloys* 7 (2014) 106-111.
- [10] A. Balińska, V. Kordan, R. Misztal, V. Pavlyuk, *J. Solid State Electrochem.* 19(8) (2015) 2481-2490.
- [11] G. Kowalczyk, V. Kordan, A. Stetskiv, V. Pavlyuk, *Intermetallics* 70 (2016) 53-60.
- [12] V. Kordan, V. Pavlyuk, O. Zelinska, *Progr. Book Abstr. XX Int. Semin. Phys. Chem. Solids*, Lviv, 2015, p. 117.
- [13] G. King, D. Schwarzenbach, *Latcon, Xtal 3.7 System*, University of Western Australia, 2000.
- [14] W. Kraus, G. Nolze, *Powder Cell for Windows*, Berlin, 1999.
- [15] <http://chem.lnu.edu.ua/mtech/mtech.htm>.
- [16] V.M. Kordan, O.I. Prokoplyuk, V.V. Pavlyuk, O.Ya. Zelinska, R.Ya. Serkiz, *Abstr. VII Nat. Conf. "Chem. Karazin's Reading"*, Kharkiv, 2016, p. 15-16.
- [17] L. Chunlei, U.E. Klotz, P.J. Uggowitzer, J.F. Löffler, *Monatsh. Chem.* 136 (2005) 1921-1930.
- [18] J.H.N. Van Vucht, H.A. Bruning, H.C. Donkersloot, A.H. Gomes de Mesquita, *Philips Res. Rep.* 19 (1964) 407-421.
- [19] A. Mendiboure, C. Delmas, P. Hagenmuller, *Mater. Res. Bull.* 19 (1984) 1383-1392.
- [20] O. Azarska, V. Pavlyuk, *Proc. X Int. Conf. Cryst. Chem. Intermet. Compd.*, Lviv, 2007, p. 42.
- [21] G.M. Zatorska, V.V. Pavlyuk, V.M. Davydov, W. Lasocha, M. Grzywa, *Progr. Book Abstr. IX Int. Semin. Phys. Chem. Solids*, Złoty Potok, Częstochowa, Poland, 2003, p. 27.